Research Journal of Chemical Sciences ISSN 2231-606X
Vol. **16(3),** 33-41, October **(2026)** *Res. J. Chem. Sci.*

Conducting Cerium and Silver doped Phosphotungstic acid–polyaniline (Ce, Ag doped PWA-PANI): A multifunctional Nanocomposite for Environmental remediation

Anjana P.T. and Preetha B*
Research Department of Chemistry, Government College, Madappally, Vadakara, 673102 Kerala, India
preethaba@gmail.com

Available online at:www.isca.in, www.isca.me
Received 12th August 2026, revised 29th September 2026, accepted 9th October 2026

Abstract

Synthesis and characterization of a conductive organic–inorganic composite, cerium and silver doped phosphotungstic acid–polyaniline composite (Ce,Ag doped PWA-PANI) is reported here. Polyaniline is incorporated into the matrices of cerium and silver doped phosphotungstic acid. The composite was prepared by simple stepwise chemical methods and characterized by using SEM, FESEM, EDAX, XRD, FTIR, XPS, UV–DRS, TGA and four–probe conductivity measurements. The studies establish a nano-sized, organic–inorganic network structure retaining the Keggin structure of the phosphotungstic acid in which Ce and Ag domains are embedded. FTIR and XPS analyses demonstrate that polyaniline and oxygen-bridged metal species are integrated within the phosphotungstate framework. Distribution studies show high selectivity towards Pb^{2+} and Th^{4+} ions, indicating its environmental application as a cation exchanger for separation and heavy-metal removal from aqueous media. UV-Visible DRS studies reveal an optical band gap of about 2.4 eV. Photocatalytic studies are performed using methylene blue as a model dye indicating efficient degradation, under optimized conditions.The composite shows relatively high and thermally stable electrical conductivity, attributed to synergistic electron and proton transport between polyaniline, Ce, Ag and phosphotungstate groups. The composite, Ce,Ag doped PTA-PANI is found very promising in environmental and electroactive applications.

Keywords: Phosphotungstic acid–polyaniline composite, selectivity, cation exchanger, photocatalytic degradation, electrical conductivity.

Introduction

Studies on conducting organic polymers are of great importance because of their ease of synthesis and fabrication, stability, controllable electrical, optical, and mechanical properties, etc., compared to prevailing inorganic materials. The synergistic action of conducting polymer composites finds wide applications in electrical, electronics, and optoelectronic areas. Structural properties greatly influence the performance of the composites[1].Synergistic outcomes resulting from the combination of polyoxometalates in conducting polymers improves the electrical conductivity, capacitance and stability of the composites[2].

Conjugated polymer like PANI conducts electricity by the electron transfer through π—π∗ interaction along its backbone structure, which can be easily tuned by an easy doping-dedoping method. Polyoxometalates consist of three or more transition metal oxyanions which are linked together by oxygen atoms, forming a large, closed 3-dimensional structure with the general formula $[M_xO_y]^{n-}$ where M = V, Mo, W, etc. By functionalizing POMs, we can prepare composite materials of different chemical and structural properties. Moreover, POMs exhibit peculiar redox properties. It was reported that $[PMo_{12}O_{40}]^{3-}$ is capable of accepting up to 24 electrons per cluster unit, leading to multi-electron transfer[4]. Electrochemical properties of POMs can be modified by fictionalization of the POM structure.

Viswanathan et al. has reported an interesting method to synthesize POM/NP/CP composites. They prepared composites of polyaniline and $[PMo_{12}O_{40}]^{3-}$ incorporating silver and gold nanoparticles. Initially, aniline was oxidatively polymerised to polyaniline by redox-active Keggin anions, $[PMo_{12}O_{40}]^{3-}$, which in turn was reduced to Keggin anion, $[PMo^{V}Mo^{VI}{}_{11}O_{40}{}^{4-}]$. Gold and silver nanoparticles were formed by the reducing action of this Kegginanion[5].

Synthesis and characterization of various composites of polyaniline–polyoxometalates were also reported which excellently catalyse the electrochemical bromate ion reduction[6]. Polyoxometalates and their composites are also found to possess cation uptake and cation exchange properties[7]. Composites of fibrous materials were also synthesized recently by the combining polymers and polyoxometalates[8]. About 10-15 nanocomposite materials were prepared by incorporating polyoxometalates in polyaniline[8].

The study here aims to prepare, characterise and evaluate the

potential applications of a conducting polymer–POX composite by incorporating a conducting polymer, polyaniline in the matrices of the cerium and silver doped phosphotungstic acid.

Materials and Methods

Synthesis of polyaniline and silver nanoparticles*:* polymerization of aniline was carried out by the chemical oxidative method, as already reported[9]. A reducing catalyst, hydrazine hydrate was used for the chemical reduction of $AgNO_3$, to prepare silver nanoparticles. To 100ml of 8 mM aqueous solution of $AgNO_3$, 0.1 M citric acid and 0.1 M NaOH solutions were introduced with vigorous stirring. In the above mixture, 20 mM hydrazine hydrate solution was added and stirred vigorously. The solution turned black after the addition of hydrazine solution which confirmed that silver ions were reduced. After 3 hours of stirring at room temperature, the solution turned transparent, which showed the production of silver nanoparticles as reported[10].

Synthesis of cerium and silver doped phosphotungstic acid-polyanilinecomposite[9]: cerium doped phosphotungstic acid was first prepared by adding 0.1 M ceric ammonium nitrate solution to 0.05M phosphotungstic acid solution with continuous stirring. A light-yellow sol of cerium phosphotungstate obtained was mixed with a definite volume of silver sol, stirred for 1 hour on a magnetic stirrer, polyaniline sol was added and stirred for one hour on a magnetic stirrer. It was kept for four hours, filtered, rinsed with deionised water, and subsequently dried.

Characterisation: Synthesized composite was characterised by SEM-EDAX, FESEM, XPS, FTIR, and UV-Visible spectroscopic studies. TGA was used to determine its thermal stability. 4-probe method was used for electrical conductivity.

Results and Discussion

The EDAX spectrum of the sample gives a plot of X-ray counts vs. energy (in keV). It is evident from the plot that there is no peak value corresponding to any impurities. The presence of cerium and silver is evident in the above EDAX spectrum, and the corresponding atomic percentages of all the expected elements are given.

Analysis of the morphology of the sample from the SEM images shows the existence of microsized particles with grain boundaries. Well-defined crystal faces are not seen. The rough texture indicates that PANI forms a continuous or semicontinuous matrix in which the inorganic domains are embedded, consistent with a hybrid organic-inorganic composite rather than a single crystalline phase. The image shows an agglomeration of particles. The individual granules are mostly in the 1-2 μm range, but these are further clustered into larger agglomerates, giving a broad polydisperse size distribution.

The observed clustered granular domains rather than large POM crystals imply that cerium and silver have likely entered the polyoxometalate framework or formed metal-oxygen linkages that stabilize smaller particles.

This is expected in this type of composites because of strong electrostatic and hydrogen bonding interactions. It suggests that the composite can favour ion exchange or catalytic activity due to the development of a continuous, interconnected network of microdomains[11].

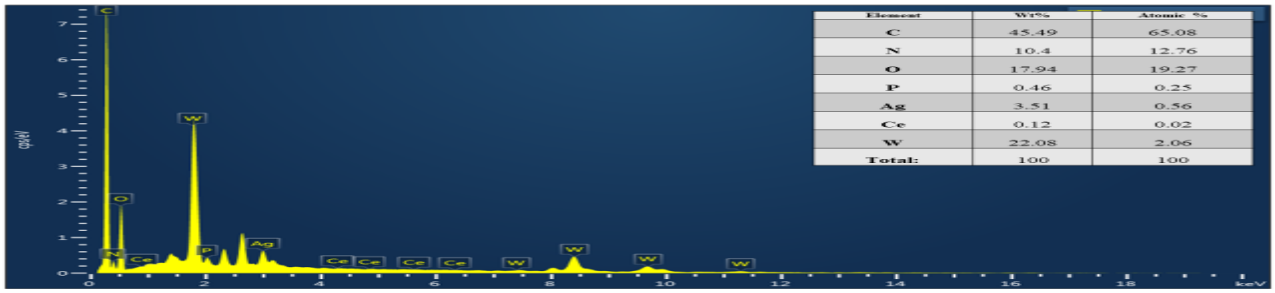


Figure-1: EDAX spectrum of Ce, Ag doped PWA-PANI

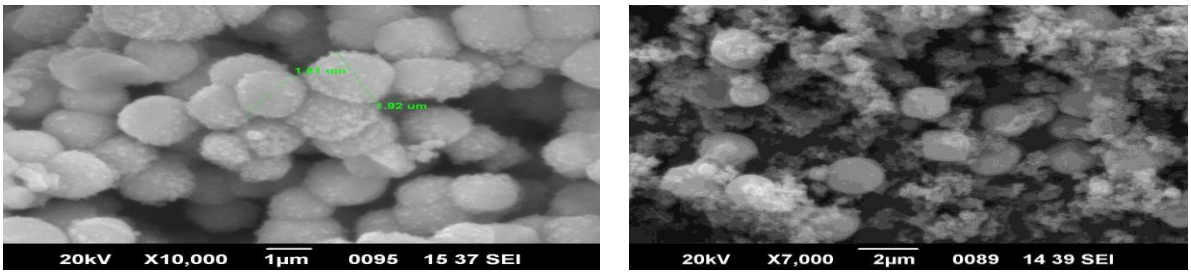


Figure-2: SEM images of Ce, Ag doped PWA-PANI.

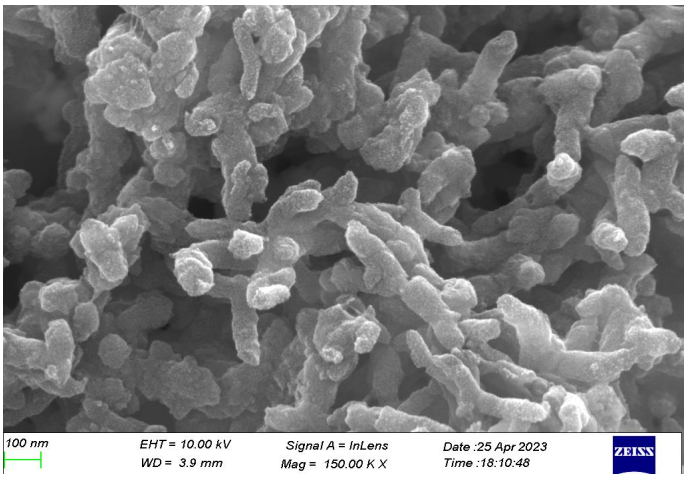


Figure-3: FESEM image of Ce, Ag doped PWA-PANI.

FESEM image shows a densely packed, interconnected columnar/ rod-like particles (indicating the presence of polyanilinefibres) of size in the nano range with rough and porous surface morphology. The individual bright spots are roughly in the 10nm range in size, while the larger aggregates extend to a few hundred nanometers. The nanosized, interconnected morphology improves the surface area, ion-exchange properties and charge-transfer phenomena[12].

Ion exchange capacity was determined by the column method[9]and was found to be 1.41 meq/g. Distribution studies with the composite were carried out for various metal ions as described earlier[9]. Distribution coefficient was determined at equilibrium as weight in mg of metal ions in 1g of composite / weight in mg of metal ions in 1ml of solution. Among the metal ions studied, the composite had highest selectivity towards Pb^{2+} and Th^{4+} (Figure-4)**.** The order of selectivity was Th^{4+} >Pb^{2+}>Zn^{2+} >Co^{2+} >Mg^{2+} >Ni^{2+}. The results showed that the material is applicable for metal ion separation and hazardous heavy metal ion elimination from contaminated water.

FTIR spectrum was taken over the range 4000 – 400 cm^{-1}showing bands from 3426 cm^{-1} to 3129 cm^{-1} attributed to symmetric and asymmetric –OH stretching and N-H stretching of the composite[13]. Figure-5 shows the presence of labile protons, as required for cationexchangers[13]. Peaks around 1578 cm^{-1} and 1486 cm^{-1} shows deformation modes of benzene rings, benzoid and quinoidrings[14], 1302 cm^{-1} shows C–N bending of vibration of aromatic amine, the peak at 1244 cm^{-1} shows C–N^{+} stretching vibrations in the polaron structure showing the existence of conducting PANI, and 1148 cm^{-1} indicates that the material contains considerable amount of polyaniline[14]. 984.38 cm^{-1} indicates W=O stretching mode of exterior WO_6 octahedron, 887.81 and 798.89 cm^{-1} represents the W–O–W stretching mode of corner and edge shared octahedron and 593.351 cm^{-1} indicates P–O bending of phosphotungsticacid[14].

The band at 508 cm^{-1} represents Ce-O vibration peak[15]. Band of Ag-O-Ag bridges shows around 500–550cm^{-1}, overlapping with PANI's C-N and aromatic vibrations. Phosphotungstic acid-PANI hybrids exhibit bands of metal-O-metal bridges around 879–890cm^{-1}, relevant for asymmetric stretching vibrations of the edge-sharing W–O–W bridges. Bridged metal-oxygen modes in the composite vibrate in the 400–900cm^{-1} fingerprint region, sensitive to doping and polymer interactions, aiding structural confirmation in POX-PANImaterials[6].

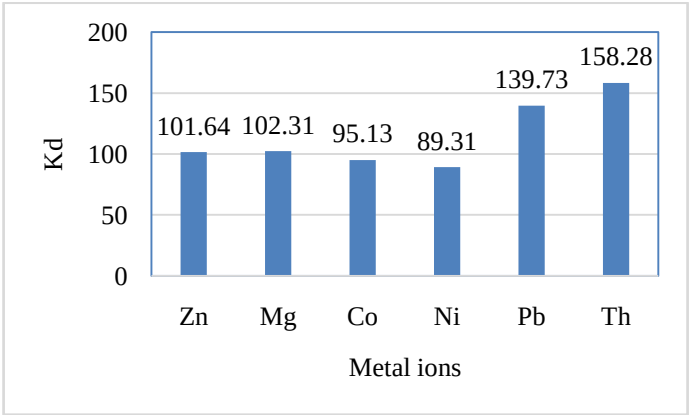


Figure-4: Distribution coefficients of metal ions.

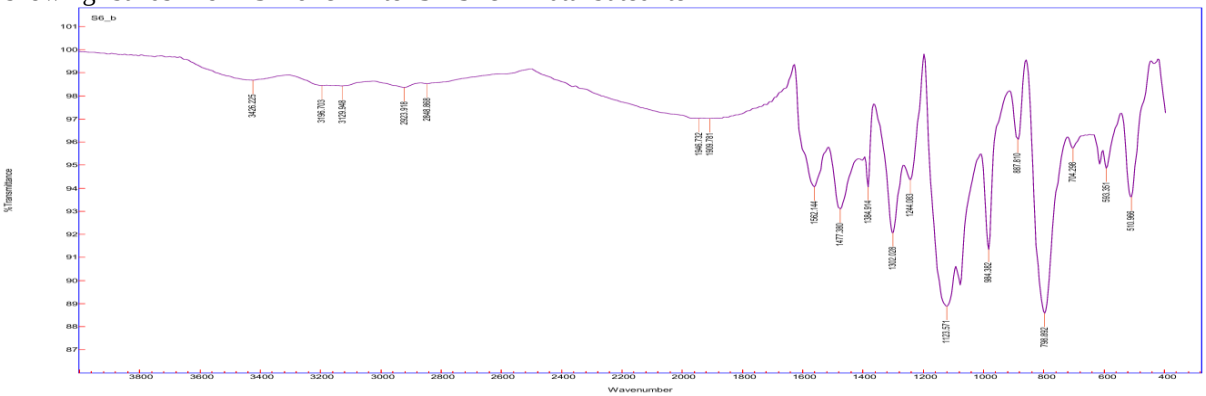


Figure-5: FTIR spectrum of the composite.

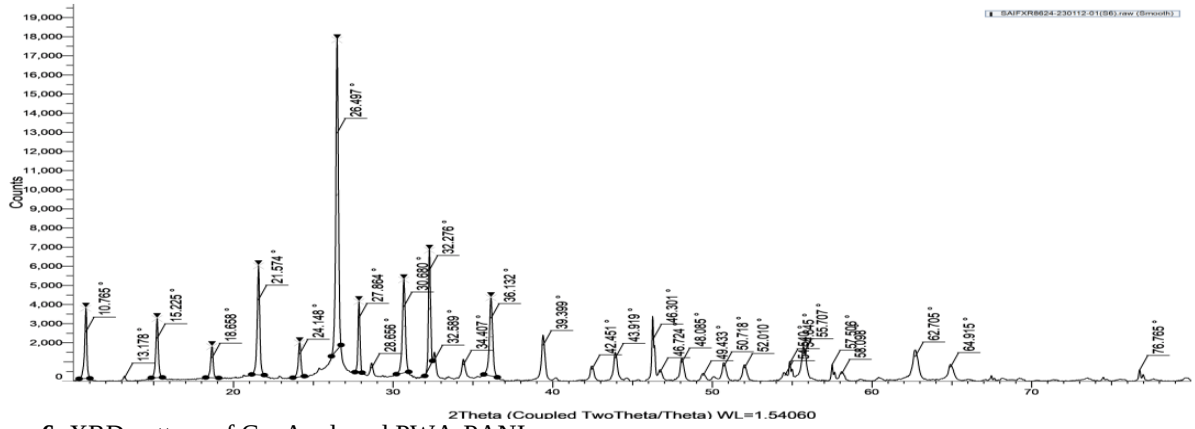


Figure-6: XRD pattern of Ce, Ag doped PWA-PANI.

Figure-6 shows the diffractogram of Ce,Ag doped PWA-PANI. Debye - Scherrer equation was used for calculating particle size. The average crystallite size was calculated as 56.35nm, revealing a nano size. The peaks around 10.765°, 15.225°, 21.574° and the strongest reflection at 2θ ≈ 26.497° in the XRD corresponds to crystalline phosphotungstic acid which indicates retention of Keggin structure. The peaks at 39.399°, 43.919°, 64.915° and 76.765° indicate the presence of dopant nanoparticles[13]. Several small medium intensity peaks in the 20-40 region correspond to PWA substructure plus crystalline domains of polyanilineemaraldinesalt[15]. The diffraction peak of PANI sharpens when it is highly doped and interacting strongly with inorganic clusters. crystallinity generally enhances charge transport and can improve photocatalytic or electrocatalyticactivity[16]. Compared with pure PANI patterns reported in literature, the shift and sharpening of peaks indicate strong interaction between PWA clusters, dopant cations (Ce, Ag), and the PANI chains, suggesting successful formation of an inorganic–organic hybrid where PWA and Ce/Ag domains are dispersed within an ordered PANI matrix.

Photocatalytic activity: Methylene blue (MB) dye was used to investigate the photocatalytic activity of the nanocomposite. Degradation capability of Ce, Ag doped PWA-PANI towards MB dye was studied. MB dye solution was prepared in deionised water. The catalytic degradation was studied by adding 500mg of photocatalyst. Using a UV–Visible spectrophotometer, absorbance was examined. Methylene blue gives absorption peaks in the visible region at 665 nm with a shoulder at 610nm.The intensity of the peaks is found to decrease with time which supports the degradation power of photocatalyst.

The absorbance was also measured by irradiating the solution with UV light at definite time intervals. The spectrum shows the degradation of the dyes. Intensity of the peak in the visible region is found to be considerably reduced. The composite removes efficiently MB dye within 90 minutes.

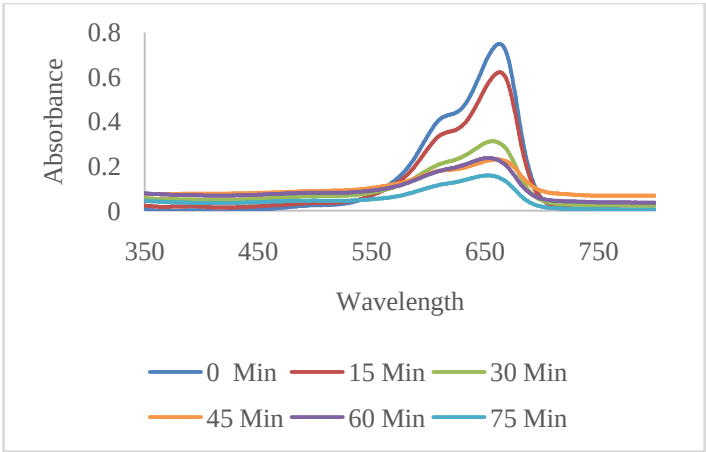


Figure-7: Absorbance spectrum of methylene blue at different time intervals.

The effect of time, amount catalyst, and pH on degradation rate was studied (Figure-8) by determining the absorbance spectrophotometrically.

Residual concentration of dye = $(C_o\text{-}C_t)$ /C_0 ×100, where C_t is concentration at time t, and C_0 is the initial concentration of dye. It was observed that degradation rate increased with increase in reaction time and catalyst dosage. The degradation rate was found to decrease in concentrated MB solutions, due to the formation of multi-layers of dye molecules on the catalyst surface. The degradation rate increased with increase in catalyst amount since surface area increases which leads to increase in active sites. pH of the dye solution affects degradation rate of the dye. pH range of 2-10 was used to study the effect on the degradation rate (Figure-8c). Dye degradation rate was found to be maximum at pH 6.

XPS spectrum of Ce, Ag, P, C, W, and O in the composite are given along with that of the composite (Figure-9). The signals corresponding to cerium, silver, and phosphorous are weak, which indicates that they are not exposed to the surface and are of low concentration.

A peak approximately at 285.5 eV represents C–C chain. Peak at 531.5 eV indicates O1s element in the composite. Peak at 37.9 eV shows that W is in the W4f5/2 state[17].

In the UV-DRS plot, several reflectance bands are observed between 200 and 380 nm in the UV region. Kubelka–Munk function is used for calculating optical band gap by plotting hvvs $(F(R)\ h\nu)^{n}$.[18] n = 1/2 for indirect forbidden gap, and n = 2 for direct allowed band. The linear portion of the curve is extrapolated to zero F(R). The band gap is about 2.4eV[18].

TGA curve (Figure-12) shows weight loss up to 100°C as external water molecules on the surface of the composite got evaporated[9]. Next decrease in weight from 100◦C to 600°C may be caused by decomposition of PANI group and condensation of groups on the surface of inorganic phases[19]. Further mass loss from 600◦C to 950◦C may be resulting from the conversion of remaining intermediate oxy-salts to more stable metal oxides and final residue[20].

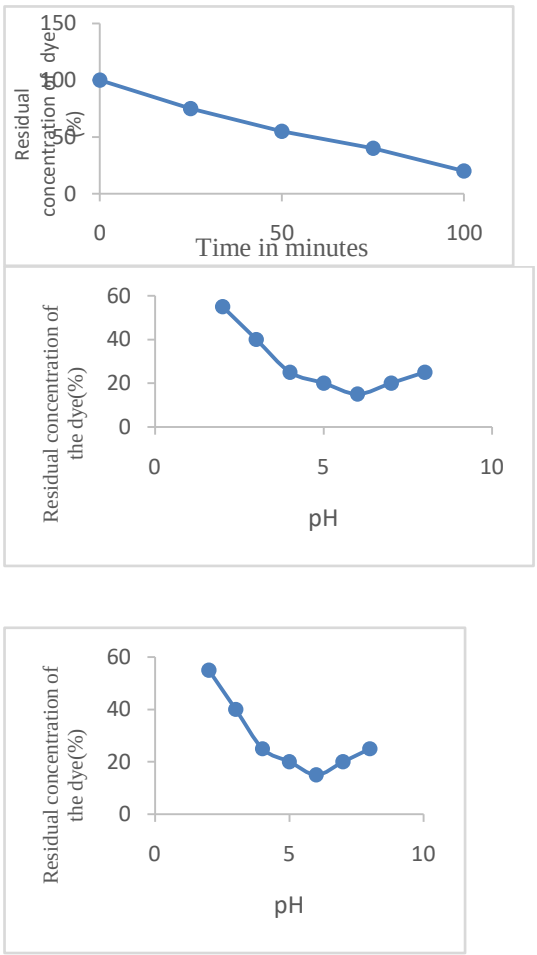
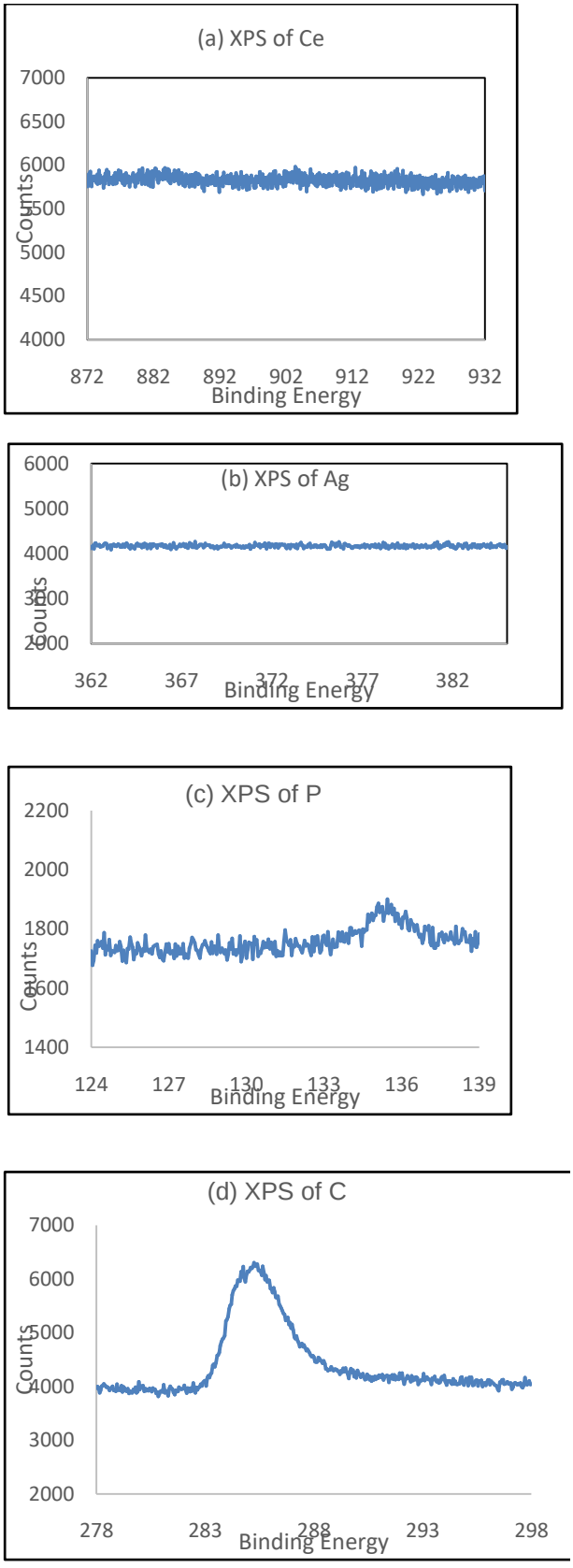
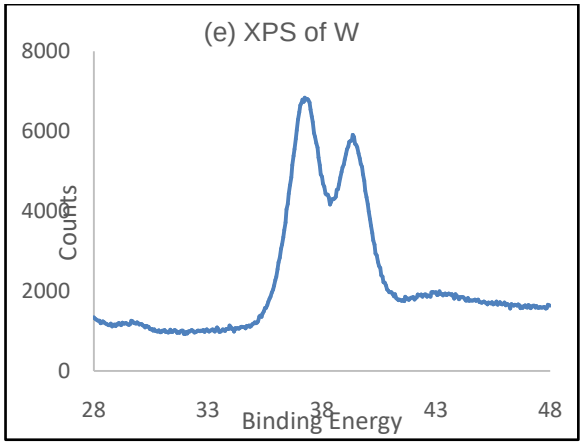
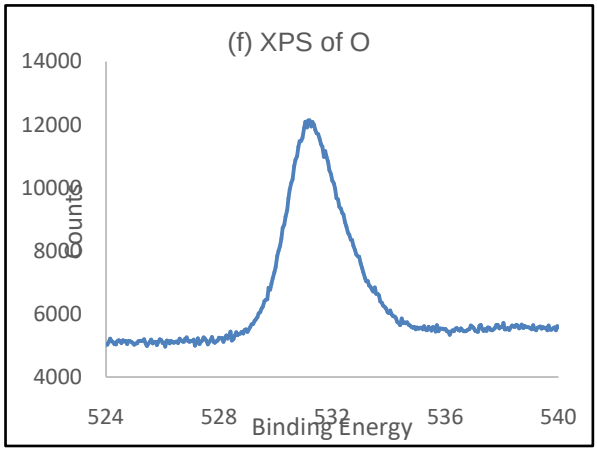


Figure-8: Effect of (a) time, (b) Amount of catalyst and (c) pH on degradation rate.







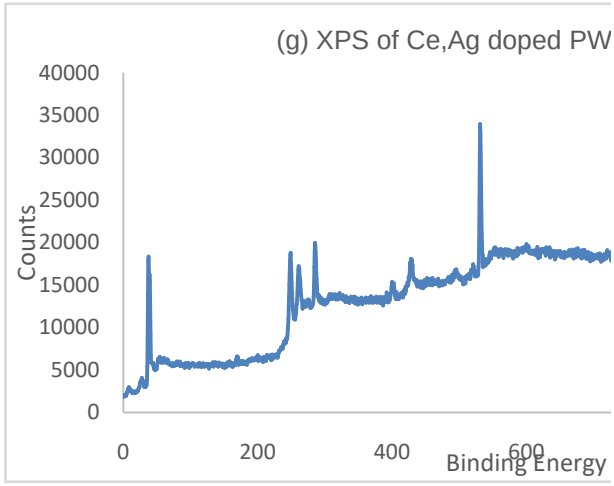


Figure-9: XPS of (a) Ag, (b) C, (c) Ce, (d) O, (e) P, (f) W, (g) Ce,Ag doped PWA-PANI.

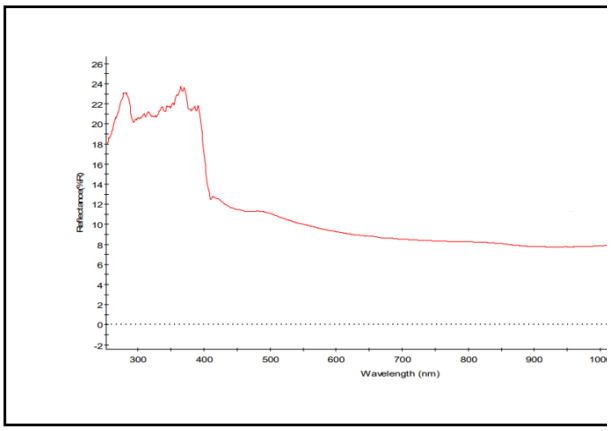
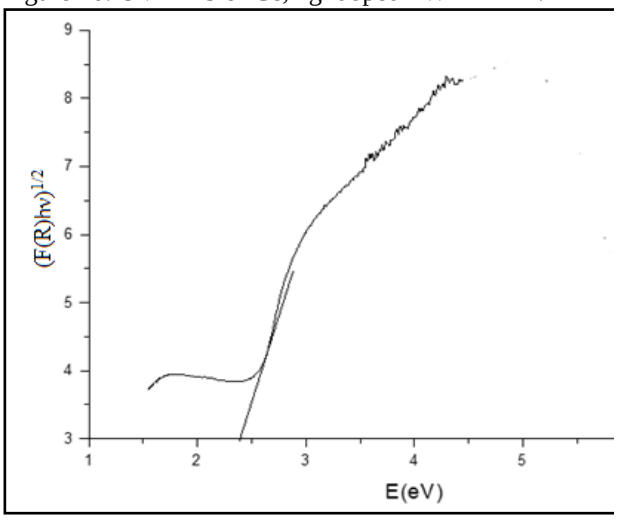


Figure 10. UV-DRS of Ce,Ag doped PWA-PANI.



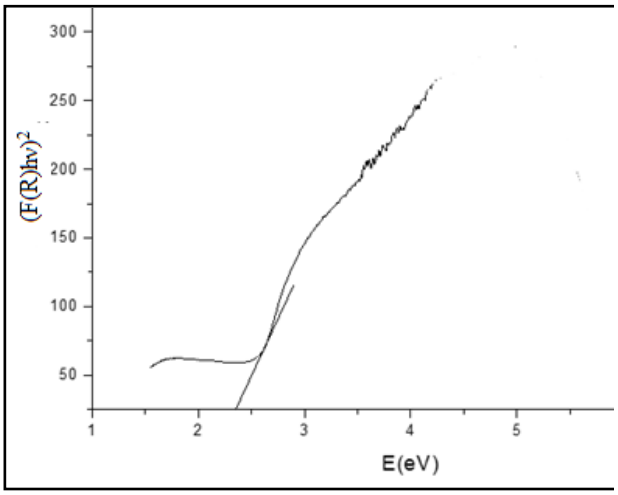


Figure-11: Band gap energy from Kubelka–Munk plot.

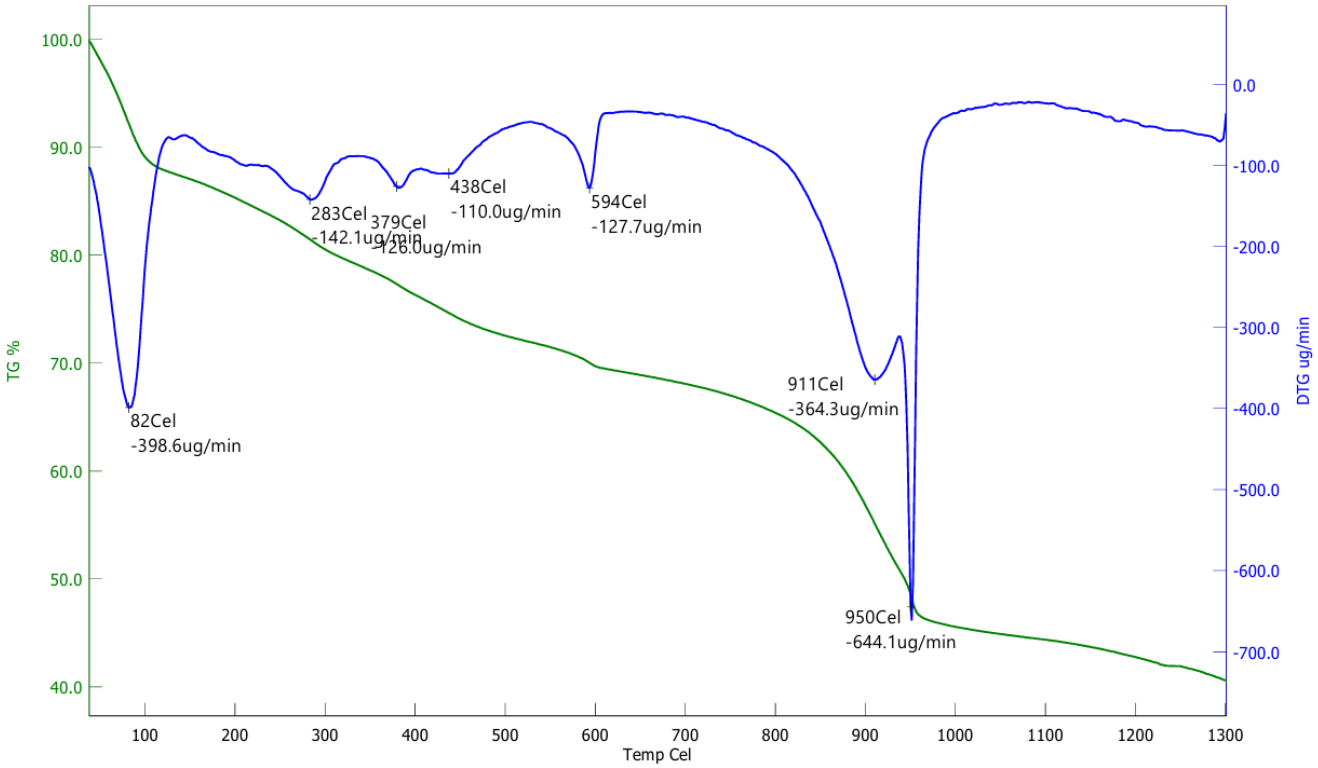


Figure-12: TGA of Ce,Ag doped PWA-PANI.

Electrical conductivities of Ce,Ag doped PWA-PANI composite pellets were studied using the four-probe method[14]. The primary constituents that are responsible for the electrical conductivity is PANI and silver. Percolation characteristic of the conducting phase is responsible for the conducting property of the composite. The electrical conductivity of the composite arises from oxidized PANI which is maintained in its conductive state by PANI-CePW/Ag counter ions. It is seen (Figure-13) that as the temperature increases, electrical conductivities increases. The values are in the range 1-4x10^{-1} S cm^{-1}, which is in the conductor -semiconductor border. The electrical conductivity measured by increasing the time showed that the electrical conductivity is quite stable at 40, 60, 80 and 100^{o}C. The electrical conductivity of Ce, Ag doped PWA-PANI is significantly high compared to that of polyaniline owing to the electron exchange property of CePW and conductivity of silver. Conductance is seen to decrease with increase intemperature. But this decreaseisless after 80^{o}C. This can be explained by considering protonic conduction at the initial stages. As temperature increases protonic conduction decreases.

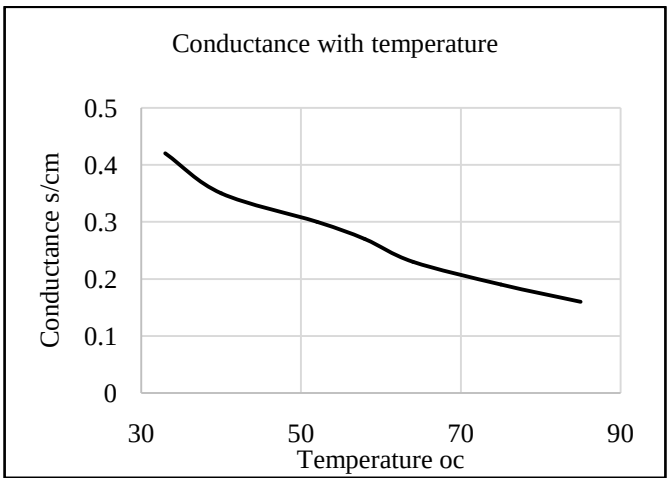


Figure-13: Variation of conductance with temperature.

Conclusion

Structurally strong, multifunctional property of conducting Ce,Ag doped PWA-PANI composite is finely established in this work. Various spectroscopic analyses reveal retention of the Keggin structure, with successful incorporation of polyaniline and oxygen-bridged metal species into a nano-structured organic–inorganic network. The material exhibits high selectivity towards Th^{4+} and Pb^{2+} in aqueous solutions, revealing its cation exchange property, and heavy metal ion sequestration from aqueous solutions. Efficient photocatalytic decomposition

of methylene blue, and an optical band gap of about 2.4 eV, reveals its potential as a visible light active photocatalyst. The composite also shows relatively high, thermally stable electrical conductivity in the 10^{-1} S cm^{-1} range, arising from synergistic electron and proton transport between PANI, CePW units, and silver. These properties demonstrate that the Ce,Ag doped PWA-PANI composite is very promising for integrated environmental and electroactive applications, including water purification, ion exchange and electroactive functional materials.

References

1. Namsheer K. and Rout C. S. (2021). Conducting polymers: a comprehensive review on recent advances in synthesis, properties and applications. *RSC Advances*, 11(10), 5659–5697.
2. Pujari Sheejal, Desai Nakul, Sudhakar Y. N., Waikard Maqsood R., Sonkawade Rajendra G., Nidhin M., and Nazareth Ronald Aquin (2025). Polyoxometalate/α-Fe_2O_3/polyaniline composite: Tailored approaches for high-performance supercapacitors. *Journal of Alloys and Compounds*, 1010, 177306.
3. Goswami Sumita, Nandy Suman, Fortunato Elvira and Martins Rodrigo (2023). Polyaniline and its composites engineering: A class of multifunctional smart energy materials. *Journal of Solid State Chemistry*, 317, 123679.
4. Herrmann Sven, Ritchie Chris and Streb Carsten (2015). Polyoxometalate–conductive polymer composites for energy conversion, energy storage and nanostructured sensors. *Dalton Transactions*, 44(16), 7092–7104.
5. Kishore P., Viswanathan B. and Varadarajan T. (2008). Synthesis and Characterization of Metal Nanoparticle Embedded Conducting Polymer–Polyoxometalate Composite. *Nanoscale Research Letters*, 3, 14–20.
6. Papagianni Grammatiki G., Stergiou Dimitrios V., Armatas Gerasimos S., Kanatzidis Mercouri G. and Prodromidis Mamas I. (2012). Synthesis, characterization and performance of polyaniline–polyoxometalates (XM12, X = P, Si and M = Mo, W) composites as electrocatalysts of bromates. *Sensors and Actuators, B: Chemical*, 173, 346–353.
7. Uchida Sayaka (2019). Frontiers and progress in cation-uptake and exchange chemistry of polyoxometalate-based compounds. *Chemical Science*, 10(33), 7670-7676.
8. Kanagaraj, J. M., Chelladurai, R., Perumal, S. & Rajamani, M. (2020). Poly(O-Toluidine) / Zirconium-based nanocomposite ion-exchangers for Water treatment and environmental remediation. *Journal of Water and Environmental Nanotechnology*, 5(1), 17–33.
9. Preetha B. (2021). Electrical Conductivity and Ion Exchange Properties of Polyaniline Antimony Tin Tungstate Nanocomposite. *Oriental Journal of Chemistry*, 37(2), 388–396.
10. Mohammad Shahjahan; Md Hasibur Rahman; Mohammad Sajjad Hossain; Most Afroza Khatun; Aminul Islam; Most Hosney Ara Begum (2017). Synthesis and Characterization of Silver Nanoparticles by Sol-Gel Technique. *Nanoscience and Nanometrology*, 3(1), 34–39.
11. Alamgeer, Tahir, M., Sarker, M. R., Ali, S., Ibraheem, Hussian, S., Ali, S., Khan, M. I., Khan, D. N., Ali, R. & Said, S. M. (2023). Polyaniline/ZnO Hybrid Nanocomposite: Morphology, Spectroscopy, and Optimization of ZnO Concentration for Photovoltaic Applications. *Polymers*, 15(2), 363.
12. Bajantri T. H., Chougale U. M., Patil S. S., Manjanna J., and Fulari Vijay J. (2024). Simple SILAR-synthesized Ni^{2+}-doped polyaniline film for supercapacitor application. *Journal of Materials Science: Materials in Electronics*, 35, 89.
13. Khan, A., Khan, A. A. P., Asiri, A. M., Rub, M. A., Azum, N. & Khan, I. (2014). Preparation, Electrical Conductivity, and Thermal Studies on Silver Doped Polyaniline Phosphotungstate Nanocomposite. *Synthesis and Reactivity in Inorganic, Metal-Organic, and Nano-Metal Chemistry*, 44(10), 1526-1530.
14. Amini Abbas, Rahimi Marjan, Nazari Marziyeh, Chenge Chun, and Samalia Bijan (2019). One-pot facile simultaneous in situ synthesis of conductive Ag–polyaniline composites using Keggin and Preyssler-type phosphotungstates. *RSC Advances*, 9, 2772.
15. Boudjelida Soufiane, Li Xue, Djellali Souad, Chiappetta Giampiero, Russo Francesca, Figoli Alberto, and Carraro Mauro (2024). Synthesis and Characterization of Polyaniline Emeraldine Salt (PANI-ES) Colloids Using Potato Starch as a Stabilizer to Enhance the Physicochemical Properties and Processability. *Materials*, 17(12), 2941.
16. Basit Maryam, Javed Sofia, GulIftikhar Hussain, Ali Zeeshan, Akram Muhammad Aftab, Shahzad Nadia, RizwanFaiza, and Islam Mohammad (2025). Polyaniline-based hierarchical heterostructures for photocatalytic degradation of organic pollutants for water treatment – A critical review. *Results in Engineering*, 28, 107967.
17. Li Ji Sen, Tang Yu Jia, Liu Chun Hui, Li Shun Li, Li Run Han, Dong Long Zhang, Dai Zhi Hui, Bao Jian Chun, and LanYa Qian (2016). Polyoxometalate-based metal-organic framework-derived hybrid electrocatalysts for highly efficient hydrogen evolution reaction. *Journal of Materials Chemistry A*, 4, 1202–1207.
18. Gesesse Getaneh Diress, Gomis Berenguer Alicia, Barthe Marie France and Ania Conchi O. (2020). On the analysis of diffuse reflectance measurements to estimate the optical properties of amorphous porous carbons and semiconductor /carbon catalysts. *Journal of Photochemistry and*

Photobiology A: Chemistry, 398, 112622.

19. Satishkumar K. B., Shashidhar, Murugendrappa M. V., Vishnuvardhan T. K. and Prabhakara S. S. (2021). Thermal analysis and conductivity of Polyanilinenanofibers - Y_2O_3 Nanocomposites. *International Journal of Research in Engineering and Science*, 9, 35–41.
20. Juan P. Yasnó, Susana Conconi and Gustavo Suárez (2022). Characterization and optical properties of m-Li_2ZrO_3 prepared by optimized solid-state reaction. *Advanced Powder Technology*, 33(3), 103514.